^{89}Y Magic-Angle Spinning NMR of $Y_2Ti_{2-x}Sn_xO_7$ Pyrochlores

Sharon E. Ashbrook,*,†,‡ Karl R. Whittle,‡ Gregory R. Lumpkin,‡ and Ian Farnan‡

School of Chemistry and EaStCHEM, University of St. Andrews, North Haugh, St. Andrews KY16 9ST, U.K., and Department of Earth Sciences, University of Cambridge, Downing Street, Cambridge CB2 3EQ, U.K.

Received: February 9, 2006; In Final Form: March 29, 2006

The yttrium local environment in the series of pyrochlores $Y_2Ti_{2-x}Sn_xO_7$ was studied using ^{89}Y NMR. Oxides with the pyrochlore structure exhibit a range of interesting physical and chemical properties, resulting in many technological applications, including the encapsulation of lanthanide- and actinide-bearing radioactive waste. The use of the nonradioactive Y^{3+} cation provides a sensitive probe for any changes in the local structure and ordering with solid solution composition, through ^{89}Y ($I = {}^1/_2$) NMR. We confirm that a single pyrochlore phase is formed over the entire compositional range, with Y found only on the eight-coordinated A site. A significant (∼15 ppm) chemical shift is observed for each Sn substituted into the Y second neighbor coordination environment. The spectral signal intensities of the possible combinations of Sn/Ti neighbors match those predicted statistically assuming a random distribution of Sn^{4+}/Ti^{4+} on the six-coordinated pyrochlore B site.

Introduction

Oxides with the pyrochlore ($A_2B_2O_7$) structure have recently generated much interest as they exhibit a range of useful properties, including both ionic and electrical conductivity, ferromagnetism, and luminescence, leading to potential technological applications as solid oxide fuel cells, electrode materials, and catalysts.[1,2] In particular, the great crystal chemical flexibility of the pyrochlore structure allowing the incorporation of a large variety of cations, coupled with the high resilience of crystalline ceramics, has encouraged utility as a host for the immobilization of nuclear waste.[3] The use of pyrochlores as components within ceramic wasteforms, such as Synroc,[4] has resulted in a focus upon the incorporation of lanthanides and actinides, and in particular of Pu, the safe disposal and long-term storage of which is currently a major concern. Primarily, titanate (i.e., B = Ti) pyrochlores have been utilized in wasteforms,[3] as a result of their high chemical durability, although recently zirconate (i.e., B = Zr) pyrochlores have been demonstrated to display an increased resistance to amorphization, i.e., the disruption of the framework structure, upon heavy ion bombardment.[3]

The pyrochlore ($A_2B_2O_7$) structure[1,5] (space group *Fd*-3*m*) is derived from that of fluorite (AO_2) through the ordered removal of one-eighth of the oxygen atoms, as shown in Figure 1a. This produces two types of possible cation species, an eight-coordinated A site, usually occupied by 2+ or 3+ cations, and a six-coordinated B site, occupied by smaller 5+ or 4+ cations. There are three distinct oxygen positions, the 48f (x, ${}^1/_8$, ${}^1/_8$), accounting for six of the seven anions per formula unit, the 8b (${}^3/_8$, ${}^3/_8$, ${}^3/_8$), and the (now) vacant 8a (${}^1/_8$, ${}^1/_8$, ${}^1/_8$). The entire structure is able, therefore, to be defined by just two variable parameters, the 48f oxygen position, x, and the cubic lattice parameter, a. The high crystal chemical flexibility of this structure, i.e., its ability to incorporate an incredibly diverse range of elements, to tolerate both cation and anion disorder, and to support variable oxidation states, is reflected in the large number (more than 500) of synthetic compositions that are known, many of which contain actinides and lanthanides.[3] The stability range of the pyrochlore phase is related to the relative sizes of the A and B cations (r_A/r_B).[1,5] It has been demonstrated when this ratio is between 1.46 and 1.78, pyrochlore structures are formed.[5] Defect fluorite structures (space group *Fm*-3*m*),

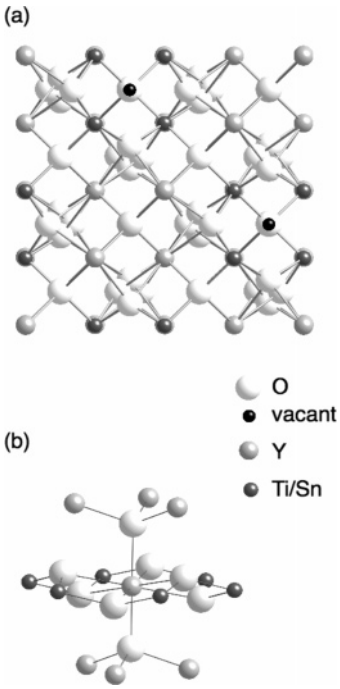

Figure 1. (a) Structure of a typical pyrochlore (projection along [110] direction). Large white spheres denote O, smaller darker spheres, the eight-coordinated A site, assumed to be occupied by Y, and the smaller dark gray spheres, the six-coordinated B site, occupied by either Ti or Sn. The smallest black spheres denote the (vacant) 8a O position. (b) Expansion showing the nearest and next nearest neighbor (NNN) environment around the eight-coordinated A site.

* To whom correspondence should be addressed. Tel: +44-1334-463779. Fax: +44-1334-46308, E-mail: sema@st-andrews.ac.uk.
† University of St. Andrews.
‡ University of Cambridge.

10.1021/jp060844q CCC: $33.50
Published on Web 05/10/2006

exhibiting both cation and anion disorder, are produced when the ratio falls below 1.46, while a considerably more complex monoclinic phase is observed when the ratio exceeds 1.78. The formation of such secondary phases is of importance, as within a wasteform, for example, they are likely to be detrimental to performance. An improved understanding of solid solution limits and of cation ordering within relevant pyrochlore phases, along with any associated effects upon physical and chemical properties, is therefore highly desirable.

In this work, we are using ^{89}Y magic-angle spinning (MAS) NMR to study the solid solution $Y_2Ti_{2-x}Sn_xO_7$, predicted by the radius ratio rules to lie within the pyrochlore stability field throughout.[5] It is assumed that the A site is occupied by the Y^{3+} cation and the B site by a distribution of $Sn^{4+}$and Ti^{4+} cations. ^{89}Y is a nonradioactive 3+ cation which has 100% natural abundance and has spin $I = {}^1/_2$, enabling high-resolution NMR spectra (free from anisotropic interactions) to be achieved through the application of MAS. Acquisition of spectra is, however, hindered by the low gyromagnetic ratio (and therefore low signal strength) of ^{89}Y and additionally by long T_1 relaxation times, often up to many thousands of seconds.[6] However, the sensitivity of NMR (and particularly of the ^{89}Y chemical shift) to subtle changes in the local electronic structure induced by cation substitution should enable the type of phases(s) formed to be identified and any limits of solid solubility to be determined. In addition, the position of Y substitution within the structure and perhaps the next nearest neighbor (NNN) Y environment can be probed, thereby also enabling a more detailed insight into cation order/disorder. This is of particular interest owing to the difficulties of diffraction on many pyrochlore systems.[2,7] For the case of X-ray diffraction, the identification of a pyrochlore phase relies on the observation of often relatively weak supercell peaks and can be hindered by the similar scattering factors of many of the constituent nuclei and the significantly weaker scattering of oxygen. Although this is not the case for neutron diffraction (where Ti for example has a negative scattering), the determination of the ordering of three or four cation species on two possible sites is not easily (if at all) achievable from a single diffraction pattern (although the unit cell size and 48f oxygen x parameter are usually well defined).[2,7] Our use of a solid solution which is anticipated to remain pyrochlore throughout should enable us to study changes in the local Y environment, free from effects related to phase transitions.

Experimental Methods

Sample Preparation. Stoichiometric amounts of Y_2O_3 (Aldrich, 99.5%), SnO_2 (Alfa-Aesar, 99.5%), and TiO_2 (Alfa-Aesar, 99.9%) were ground together in an agate ball mill using acetone as a mobile phase. Once dried, the powders were pressed into pellets and calcined at 1500 °C for 48 h at a heating rate of 10 K min^{-1}, cooled, reground, and pressed into pellets prior to a further heating at 1500 °C for a further 96 h. Once calcined, the samples were ground into a powder sufficient to pass through a 38 μm filter.

Sample Characterization. *X-ray Diffraction.* Samples were examined using a Bruker D8 diffractometer with monochromatic Cu Kα_1 radiation (1.5406 Å) and a tuned Sol-X detector. The angular range used was 10−80° 2θ, corresponding to a d spacing range of 1.198−8.835 Å, with a step size of 0.01° and a counting time of 5 s. All samples were shown to be single phase, exhibiting a classical pyrochlore diffraction pattern, as shown in Figure 2a. The unit cell parameter, a, was determined using EXPGUI/GSAS[8,9] and a Le-Bail refinement. The change in unit cell size was found to be linear with composition, increasing from titanate[10] to stannate,[11] as shown in Figure 2b in agreement with the literature.

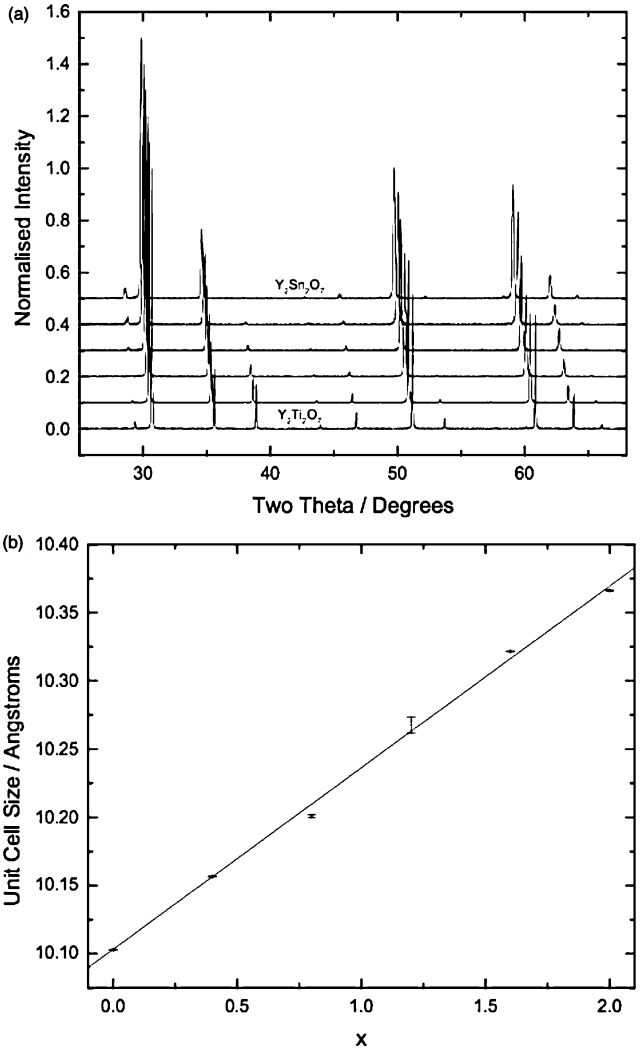

Figure 2. (a) X-ray diffraction patterns for $Y_2Ti_{2-x}Sn_xO_7$ (x = 0, 0.4, 0.8, 1.2, 1.6, and 2) showing the single phase pyrochlore nature of the materials. (b) Plot of the change in the unit cell size as a function of solid solution composition, x.

Electron Microscopy. The microstructures, diffraction patterns, and chemical compositions were investigated by electron microscopy. Polished sections were examined by scanning electron microscopy (SEM) using a JEOL 6400 operated at 15 kV and equipped with a Noran Voyager energy-dispersive X-ray (EDX) analysis system. Samples were prepared for transmission electron microscopy (TEM) by the grinding in methanol of small portions of the powders used in the NMR experiments, followed by deposition of the suspended particles onto 3 mm diameter holey carbon/copper grids. Several crystal fragments of each sample were studied by electron diffraction using a JEOL 2000fxII operated at 200 kV. A Gatan double tilting sample holder was employed in order to bring the individual crystals into zone axis diffraction conditions. The camera constant of this instrument was calibrated over a range of objective lens current settings using a polycrystalline gold standard.

Secondary electron images showed that the sintered samples have substantial porosity, but this decreases systematically with Ti content. Backscattered electron images suggest that the samples are reasonably homogeneous, with only slight variation in composition for the samples with x = 0.4, 0.8, and 1.2. A

TABLE 1: SEM−EDX wt % Analyses and Chemical Formulas Based on 7.00 Oxygens for $Y_2Ti_{2-x}Sn_xO_7$ Pyrochlores

	$x = 0.0$	$x = 0.4$	$x = 0.8$	$x = 1.2$	$x = 1.6$	$x = 2.0$
TiO_2	41.0	31.7	23.2	14.6	7.4	0.0
SnO_2	0.5	14.6	26.1	39.0	47.2	56.7
Fe_2O_3	0.1	0.0	0.1	0.2	0.1	0.1
Y_2O_3	58.4	54.3	51.4	48	45.4	42.6
Ti	1.98	1.62	1.26	0.84	0.46	0.00
Sn	0.01	0.4	0.75	1.17	1.55	2.00
Fe	0.01	0.00	0.01	0.01	0.01	0.01
sum B	2.00	2.02	2.03	2.03	2.03	2.01
Y	2.00	1.97	1.98	1.97	1.98	1.99

survey of the chemical composition of all samples in the series was conducted using EDX, and results indicate that the samples are, on average, close to their nominal compositions (see Table 1). The Ti and Sn contents vary by up to ∼0.05 atoms per 7 oxygens, in the three samples noted above, confirming the zoning noted in the backscattered electron images. All four of the intermediate compositions ($x = 0.4-1.6$) also have a slight deficiency in Y and excess in the B-site total, but these values are within 2 standard deviations of their ideal values. All samples were determined to be essentially single phase; however, the presence of a minor phase was noted in some of the backscattered electron images. EDX spectra suggest that this is yttrium silicate, but the grain size is too small for accurate analysis. This phase comprises no more than 2−3 vol. % of the samples in which it was observed. Electron diffraction results indicate that all of the samples possess the ordered pyrochlore structure. Selected area diffraction patterns for the [110] zone axis in each sample, shown in Figure 3, closely resemble calculated pyrochlore diffraction patterns for typical thicknesses of 50−100 nm. The lack of any diffuse scattering indicates no evidence for domains due to local order−disorder deviations for any composition.

NMR Spectroscopy. NMR spectra were acquired using a Varian Infinity Plus 500 MHz spectrometer, equipped with a wide-bore 11.7-T magnet, operating at 24.5 MHz for ^{89}Y. Powdered samples were packed into 7.5-mm silicon nitride rotors (to ensure no background Y signal from the rotor itself) and rotated (when applicable) at rates up to 6.5 kHz in a commercial probe with a low-γ tuning attachment. Radio frequency field strengths of ∼20 kHz were used, resulting in 90° pulse lengths of 10−12 μs. Preacquisition delays of 60−100 μs were also used in order to eliminate probe ringdown.

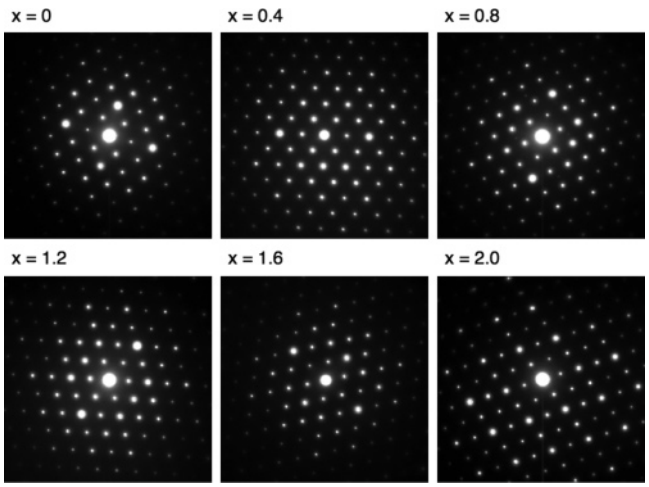

Figure 3. Selected area electron diffraction patterns for $Y_2Ti_{2-x}Sn_xO_7$ pyrochlores for $x = 0$, 0.4, 0.8, 1.2, 1.6, and 2.

Spectra were acquired using small (∼π/5) flip angle pulses enabling shorter recycle intervals to be used, although when accurate spectral integration was required much longer intervals were also employed. When samples were static, spectra were acquired using a Carr−Purcell−Meiboom−Gill (CPMG)[12] echo train to improve sensitivity, with a long recycle interval. Echoes were co-added prior to Fourier transformation. Chemical shifts are shown relative to 1 M YCl_3(aq) and measured using a $Y_2Ti_2O_7$ as a secondary reference at 65 ppm.[6] Spectral analysis and fitting were performed within the dmfit[13] program. Line shapes were constrained to be Lorentzian as this gave the best quality of fit (no significant improvement was obtained when the Gaussian/Lorentzian character was allowed to vary). No further constraints were applied. Any further details are given in figure captions.

Results and Discussion

Conventional ^{89}Y MAS NMR spectra of $Y_2Ti_2O_7$ and $Y_2Sn_2O_7$ are shown in parts a and d of Figure 4. A single, sharp resonance is observed in each case, at isotropic chemical shifts, δ_{CS}, of +65 and +150 ppm, respectively, along with spinning sidebands in the case of the titanate, in good agreement with previous results.[14] This confirms the presence of a single well-ordered pyrochlore phase with one crystallographically distinct Y species, located on the eight-coordinated A site. A general relationship of increasing chemical shift with decreasing coordination number has been observed for a range of Y-containing materials.[15,16] It may be expected, therefore, that any substitution of Y onto the six-coordinated B site would result in a resonance at much higher chemical shift. While this is a reasonable assumption within the context of these materials, it should be noted that the large shift range of ^{89}Y and strong dependence of δ_{CS} upon local structure do restrict the more general use of this empirical relationship.[14−17] This sensitivity to the local environment is evidenced by the significant difference in chemical shift (∼85 ppm) between the titanate and stannate pyrochlores, resulting from the different next nearest neighbor interactions. When the B site is occupied by the higher field strength (Z/r), more polarizing Ti^{4+} cation, the resonance is substantially shifted upfield (i.e., to lower ppm).

The anisotropy of the ^{89}Y chemical shift can be determined from the slow MAS and static spectra also shown in Figure 4. For static samples, a CPMG[12] echo train was employed in order to increase sensitivity, with the echoes co-added prior to Fourier transformation. A much larger chemical shift anisotropy is observed for $Y_2Ti_2O_7$ ($\Delta_{CSA} = -390$ ppm, $\eta_{CSA} = 0.05$) than for $Y_2Sn_2O_7$ ($\Delta_{CSA} = -135$ ppm, $\eta_{CSA} = 0.08$), again in agreement with literature values.[14] Computer-generated line shapes, simulated using these parameters, are also shown in Figure 4. The differences in anisotropy are due to the oxygen 48f x parameters for the two, both of which differ from the ideal value found in fluorite (0.375), with $x = 0.338$ for yttrium stannate[11] and 0.327 for yttrium titanate.[10] Deviation of x away from 0.375 results in a distortion of the oxygen coordination around each Y from that of an ideal cube. This distortion is greater for $Y_2Ti_2O_7$, resulting in a larger anisotropy.

For both materials, the ^{89}Y longitudinal (or spin−lattice relaxation) time, T_1, as measured by saturation-recovery experiments is fairly long, although substantially shorter than the T_1 values for Y_2O_3 and related sulfur compounds where values of up to 24 000 s were observed.[17] The stannate pyrochlore spin−lattice relaxation was slightly slower than that of the titanate pyrochlore. The T_1 values are in general agreement with those previously reported for diamagnetic pyrochlores, although

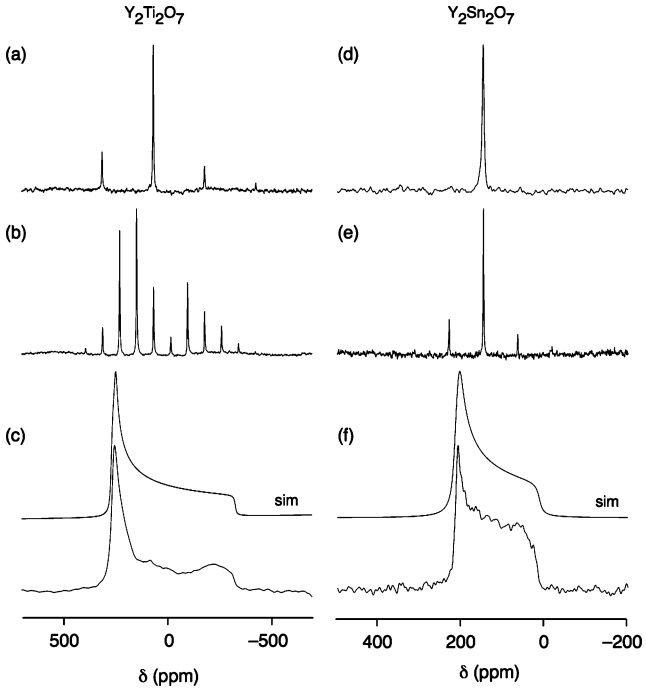

Figure 4. ^{89}Y (24.5 MHz) (a, b, d, e) MAS and (c, f) static NMR spectra of (a−c) $Y_2Ti_2O_7$ and (d−f) $Y_2Sn_2O_7$. Spectra are the result of averaging (a) 128, (b) 400, (c) 128, (d, e) 120, and (f) 228 transients with recycle intervals of (a) 10 s, (b) 30 s, (c) 1500 s, (d, e) 10 s, and (f) 1500 s. For static samples, spectra were acquired using a CPMG echo train consisting of 30 echoes (and a frequency domain spacing $1/\tau$ of (c) 125 Hz and (f) 100 Hz). Echoes have been co-added prior to Fourier transformation. The MAS rate was (a) 5.2 kHz, (b, e) 2 kHz, and (d) 6.0 kHz. Chemical shifts are relative to 1 M YCl_3(aq). In (c, f) a computer-generated fit is also shown, simulated with parameters (c) $\delta_{CS} = 65$ ppm, $\Delta_{CSA} = -390$ ppm, and $\eta_{CSA} = 0.05$ and (f) $\delta_{CS} = 150$ ppm, $\Delta_{CSA} = -135$ ppm, and $\eta_{CSA} = 0.08$, as determined by line shape fitting.

substantially shorter values were observed for pyrochlores containing paramagnetic Ln^{3+} cations substituted onto the A site.[14] The T_1 recovery behavior is nonexponential as is often found for relaxation by paramagnetic impurities.[18] Full recovery of the equilibrium magnetization is achieved between 2500 and 6000 s, which we can estimate to be approximately 5 T_1.

The ^{89}Y MAS NMR spectra across the compositional range of the $Y_2Ti_{2-x}Sn_xO_7$ solid solution are shown in Figure 5. Each spectrum exhibits fairly sharp resonances within the 60−160 ppm range observed for the two end members, confirming a pyrochlore phase is present. There does not appear to be any Y substitution onto the B site (producing a resonance at higher chemical shift as described previously). The low intensity peak observed when $x = 1.2$ at ∼180 ppm, denoted *, is assumed to result from an artifact as it was not reproduced consistently. The single resonances for the pure end members are generally narrower than the peaks observed throughout the series, probably reflecting the increase in the longer range disorder as the pyrochlore B site becomes occupied by both Sn and Ti. Throughout the solid solution a range of resonances are observed, assumed to result from the presence of different numbers of Sn and Ti on the neighboring B sites.[14] Figure 1b shows the nearest and next nearest neighbor environment around the eight-coordinated pyrochlore A site, shown occupied by Y, with six B site NNN (at distances of 3.66 Å for B = Sn[11] and 3.57 Å for B = Ti[10]) and six A site neighbors, three above and three below. As substitution of Sn for Ti takes place throughout the solid solution there are seven possible local environments, which depend on the number of Sn on the six surrounding B

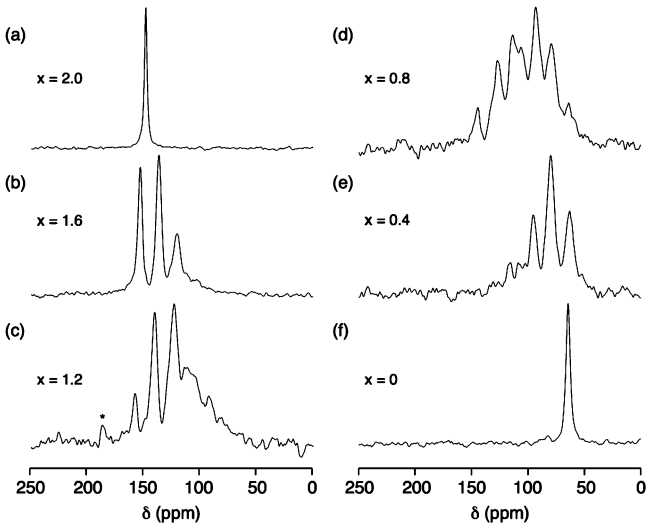

Figure 5. ^{89}Y (24.5 MHz) MAS NMR spectra of $Y_2Ti_{2-x}Sn_xO_7$ where $x = 0$, 0.4, 0.8, 1.2, 1.6, and 2. Spectra are the result of averaging 80 transients with a recycle interval of 5000 s. The MAS rate was 6.0 kHz. Chemical shifts are relative to 1 M YCl_3(aq). The peak denoted * when $x = 1.2$ is an artifact.

sites, from 0 Sn NNN (as in $Y_2Ti_2O_7$ at 65 ppm) to 6 Sn NNN (as in $Y_2Sn_2O_7$ at 150 ppm). As an example, when $x = 1.6$ ($Y_2Ti_{0.4}Sn_{1.6}O_7$) three intense resonances are observed corresponding to three distinct Y environments (Figure 5b). The peak at highest chemical shift (∼154 ppm) is similar to that found in $Y_2Sn_2O_7$ and results from 6 Sn NNN. Two further peaks at ∼137 ppm and ∼122 ppm result from 5 Sn/1 Ti and 4 Sn/2 Ti NNN, respectively, indicating a chemical shift change of ∼14−15 ppm from the substitution of a single Ti. Interestingly, the resonance assigned to 6 Sn NNN in $Y_2Ti_{0.4}Sn_{1.6}O_7$ displays a small but significant shift (downfield) from that found in $Y_2Sn_2O_7$. In addition to changes in the NNN environment, substitution of Ti for Sn also decreases the average size of the B cation and results in both a decrease in the unit cell size (as shown in Figure 2b) and a change in the oxygen 48f x position.[2] It has been noted previously that such a change can also result in a chemical shift.[19] In this case the shift is much smaller in magnitude (∼4 ppm) than that brought about by the NNN changes and is in the opposite sense. This effect appears more pronounced at the Sn-rich end of the solid solution

As described above, a comparison of the spectra in Figure 5 with $Y_2Sn_2O_7$ allows the environment corresponding to 6 Sn NNN to be identified (∼150 ppm) and for $x = 1.6$ both 5 Sn (∼135−145 ppm) and 4 Sn (∼120−130 ppm) NNN resonances are clear. Similarly, a comparison with $Y_2Ti_2O_7$ identifies 0 Sn NNN (∼65 ppm) and from the spectrum when $x = 0.4$ peaks corresponding to 1 Sn (∼78−83 ppm) and 2 Sn (∼90−95 ppm) NNN can be identified. However, two unidentified resonances remain in the set of spectra with shifts of ∼109−115 ppm and ∼100−105 ppm. This can be seen more clearly in Figure 6 where the NMR spectra for $x = 1.2$ and $x = 0.8$ are shown, with the peak assignment (number of Sn NNN), in more detail. (Closer examination of Figure 5 also reveals the presence of two such peaks in the $x = 1.6$ and 0.4 spectra also.) One possible explanation involves the presence of two phases at some or all compositions in the solid solution, with perhaps exsolution into Sn-rich and Ti-rich phases (both of which are pyrochlore and so are not easily distinguished by diffraction). However, such a conclusion is not supported by microscopy and diffraction, where there is no evidence for the formation of two such phases. Perhaps a simpler explanation is the assignment of both resonances to an environment with 3 Sn/3 Ti NNN but with a

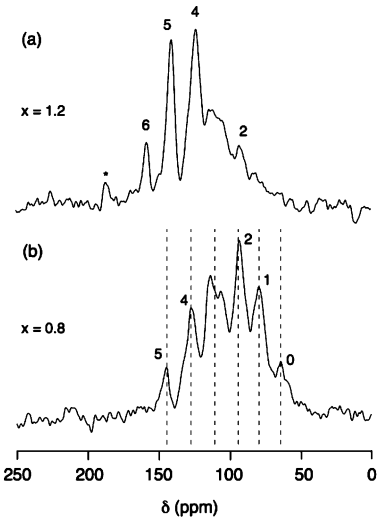

Figure 6. Expansion of ^{89}Y (24.5 MHz) MAS NMR spectra of $Y_2Ti_{2-x}Sn_xO_7$ for $x = 1.2$ and 0.8 shown in Figure 5. Peak assignments (number of Sn NNN) are given. In (b), gray dashed lines show the predicted position of resonances based on a 14−16 ppm chemical shift on Sn/Ti substitution.

differing spatial arrangement of these neighbours on the six surrounding B sites. Such an assignment is supported by the observed chemical shift change upon the substitution of a single Sn or Ti, which would predict the resonance corresponding to 3 Sn NNN to lie approximately in the center of the two peaks, as shown in Figure 6b. It is easy to envisage the origin of differing spatial arrangements from a consideration of the cluster shown in Figure 1b, where the Sn atoms may be arranged adjacent to each other on the 6 B sites, or some or all spaced by Ti. Such differences may produce small but observable changes in shift, resulting in a broadening or splitting of resonances. Obviously, this effect is not confined only to 3 Sn NNN, and it should be noted that some other resonances in Figure 5 do exhibit significant shoulders. It is difficult to determine in any more detail such splittings/shoulders, owing to both the overlap of peaks and the reasonably low signal-to-noise ratio (despite the 4.5 day acquisition time). As a final consideration, it should perhaps be mentioned that small differences in chemical shift may also arise from longer range effects, although it would be surprising if this resulted in such an obvious splitting as many such possibilities exist. The more obvious consequence would be the increase in peak width (compared with that found for the end members), as described previously.

The relative (integrated) intensities of the resonances (and any spinning sidebands) in the spectra in Figure 5 should, in theory, provide information about the distribution of Sn and Ti across the B sites, i.e., cation order/disorder, in each compound. As discussed in the Introduction, this is of particular interest owing to the problems encountered with diffraction, and because of the importance of this effect in determining microstructure, physical and chemical properties, radiation resistance, and even phase transitions. A vital prerequisite, however, is that the relative spectral intensities accurately reflect the relative site populations, i.e., that the recycle interval is sufficient. It is well known that long T_1 relaxation times are common for ^{89}Y[17] and those for $Y_2Ti_2O_7$ and $Y_2Sn_2O_7$ were discussed earlier. Figure 7 shows a T_1 saturation-recovery experiment for $Y_2Ti_{0.4}Sn_{1.6}O_7$ ($x = 1.6$). A consideration of the three main resonances reveals that while T_1 is long (∼1000−2000 s) little relative relaxation is observed between the resonances even at shorter τ. The acquisition of spectra with variable recycle intervals revealed

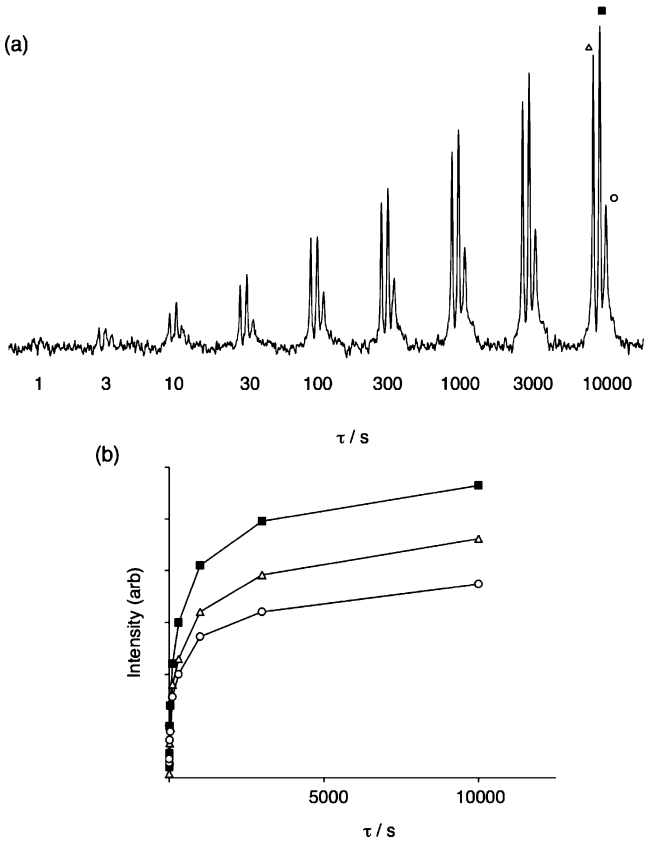

Figure 7. (a) ^{89}Y (24.5 MHz) MAS NMR spectra of $Y_2Ti_{0.4}Sn_{1.6}O_7$ ($x = 1.6$), recorded using a saturation-recovery experiment as a function of relaxation time interval, τ. (b) Plot of ^{89}Y integrated signal intensity (arbitrary units), extracted from the spectra in (a) for each of the three distinct resonances as a function of τ and denoted by open triangles, filled squares, and open circles in order of decreasing chemical shift.

that accurate relative intensities could generally be obtained with recycle intervals above 3000 s.

It is possible, therefore, to compare the intensities obtained by experiment for each NNN environment to those predicted theoretically if the distribution of Sn and Ti on B was random. For the case of 3 Sn NNN the integrated intensities of both of the two peaks discussed previously were combined. A simplified model is used, considering only the NNN coordination environment around each Y (as shown in Figure 1b). As suggested by the NMR spectra, it is assumed that Y occupies only the A site, while the six surrounding B sites are assumed to be occupied by a random distribution of Sn and Ti, with nominal compositions used. The probability of finding a Sn NNN in $Y_2Ti_{2-x}Sn_xO_7$ is simply given by $p = x/2$. No account is taken of any further topology in the system, i.e., how the clusters in Figure 1b are connected in the three-dimensional framework. It can be shown by simple statistics that the probability of finding n Sn NNN, $P(n\ \mathrm{Sn})$, is then given by a binomial distribution

$$P(n\ \mathrm{Sn}) = \Omega\, p^n\, (1-p)^{6-n} \qquad (1)$$

where Ω is the number of permutations, i.e., the number of possible ways n Sn can be arranged upon the six sites, i.e., 1 for $n = 0$, 6 for $n = 1$, 15 for $n = 2$, etc. For example, in $Y_2Ti_{0.4}Sn_{1.6}O_7$ $x = 1.6$, $p = 0.8$ and so the probability of 4 Sn NNN is given by

$$P(4\ \mathrm{Sn}) = 15\ (0.8)^4\ (0.2)^2 = 0.245 \qquad (2)$$

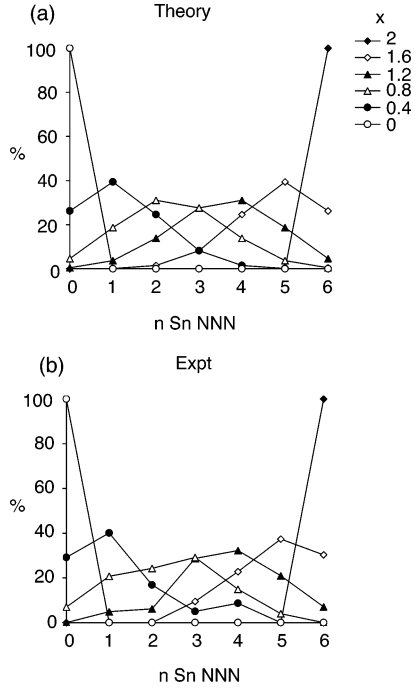

Figure 8. Plot of signal intensities (expressed as %) for (a) a statistical model assuming a random distribution of Sn/Ti on the pyrochlore B site and (b) extracted from ^{89}Y (24.5 MHz) MAS NMR spectra of $Y_2Ti_{2-x}Sn_xO_7$, as a function of the number of Sn NNN. Open circles, filled circles, open triangles, filled triangles, open diamonds and filled diamonds signify $x = 0$, 0.4, 0.8, 1.2, 1.6, and 2, respectively.

That is, we would expect 24.5% of the spectral intensity to be found in the resonance assigned to 4 Sn NNN. Experimentally we find that the resonance assigned this environment accounts for 22.8% of the spectral intensity.

A comparison of the intensities predicted using this model and those obtained experimentally is shown in Figure 8, plotted as a function of the number of Sn NNN for varying solid solution compositions, *x*. Very good agreement is observed, which, given the assumptions in the model, the peak overlap/splittings observed experimentally, and the relative poor signal strength of ^{89}Y NMR, is perhaps surprising. The agreement is seen more clearly in Figure 9, where the experimental and theoretical intensities are compared for each NNN environment, as a function of solid solution composition. Only small differences are observed, particularly for 2 and 4 Sn NNN, indicating there is no reason to suppose the Sn/Ti distribution across the B sites is anything other than random. The small differences observed probably result from the experimental overlap of peaks (particularly those in the center of the spectra where splittings and shoulders are more prominent) and perhaps the simplified nature of the model. The agreement also possibly provides support for the assignment of the two previously unidentified resonances both to 3 Sn NNN. It is perhaps useful also to consider the alternative situation, where the Sn/Ti distribution is not random. There are two cases, avoidance or clustering, where the probability of finding a (say) Sn NNN to a Y is substantially reduced or increased, respectively, if one is already present. In the extreme case of the former, 1 Sn NNN would be very common at low Sn content, with 2, 3, etc., only possible once the Sn content was sufficiently high. For the case of clustering, primarily low (0) and high (5, 6) numbers of Sn NNN would be expected at the expense of intermediate values. The experimental evidence is clearly far from these two situations.

It has been reported that in the synthesis of similar oxide pyrochlore systems, some of which undergo phase transitions to a defect fluorite phase, the structure and ordering of the material produced are strongly dependent upon the synthesis method, with an equilibrium structure difficult to achieve as a result of slow cation diffusion rates.[2,20] However, in this case, the stochastic B cation mixing evidenced by ^{89}Y NMR indicates that in all likelihood the equilibrium state has been achieved and cation diffusion is not a factor, at least for the synthesis temperature used here. For other systems, ^{89}Y (or ^{17}O) NMR may be an essential tool in the investigation of structural changes with synthesis type (e.g., solid state, sol−gel) and/or calcination

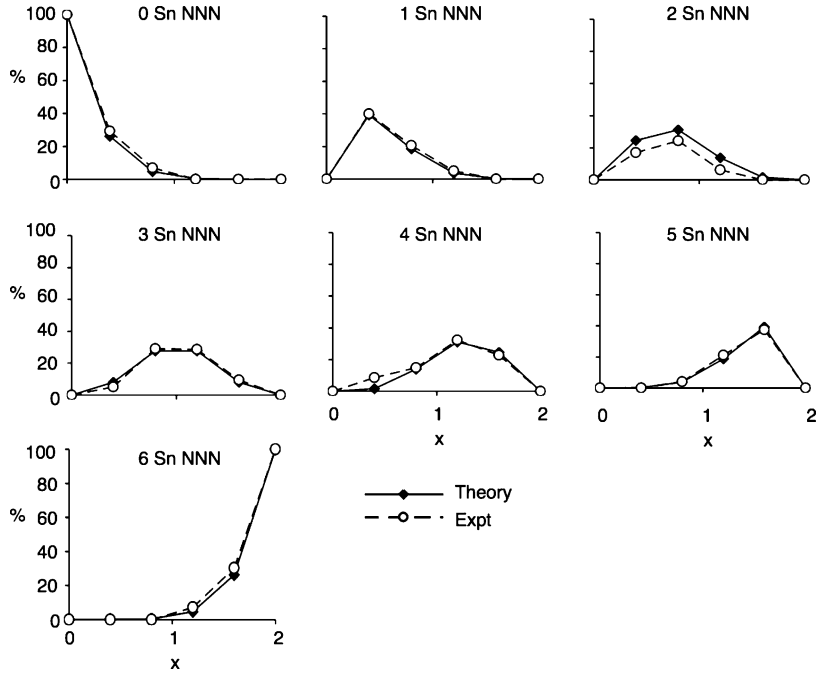

Figure 9. Plot of signal intensities (expressed as %) for each type of NNN environment as a function of solid solution composition, *x*, for the pyrochlores $Y_2Ti_{2-x}Sn_xO_7$. Both theoretical (filled diamonds, solid line) and experimental (open circles, dashed line) intensities are shown, with the latter extracted from ^{89}Y (24.5 MHz) MAS NMR spectra.

temperature, owing its sensitivity to subtle changes in the local environment around Y (or O), which may be difficult to determine by diffraction. It should be noted that ^{17}O NMR has already been successfully used to characterize local environments in titanate, stannate, and zirconate pyrochlore systems.[21,22]

Conclusions

We have demonstrated that ^{89}Y NMR is an excellent probe of the cation local environments in the solid solution $Y_2Ti_{2-x}Sn_xO_7$, with great potential for the investigation of structure−property relationships in these and similar materials. Despite low signal strength (low γ) and long T_1 relaxation times, spectra can be obtained on a practical time scale at moderately high (i.e., 500 MHz) field strengths with sufficient signal to noise and resolution. Our results confirm the conclusions from diffraction and microscopy that the solid solution remains single phase pyrochlore throughout. NMR also provides information on cation ordering, suggesting that Y occupies only the eight-coordinated A site, while the six-coordinated B site is most probably occupied randomly by Sn and Ti atoms. The large chemical shift change (∼15 ppm) upon the substitution of Sn or Ti into the NNN environment allows resonances corresponding to the different possible environments to be distinguished. Smaller shift changes resulting from changes in the unit cell parameter are also observed. The presence of more than seven resonances (from the seven possible NNN environments) was ascribed to differences in chemical shift resulting from different spatial arrangements. It is possible that a more detailed analysis could be performed if a higher spectral resolution was obtained. Perhaps the most obvious approach would be the use of higher B_0 field strengths, although it is possible that peak widths may also increase if they are dominated by inhomogeneous (e.g., chemical shift distribution) rather than homogeneous (e.g., relaxation) broadening. The use of ab initio calculations may also prove beneficial, although the unit cells involved are reasonably large, especially when disorder is considered.

Acknowledgment. S.E.A. thanks the Royal Society for a Dorothy Hodgkin Research Fellowship. The Cambridge Centre for Ceramic Immobilization (C3i), the Cambridge−MIT Institute (CMI), and British Nuclear Fuels (BNFL) are thanked for funding. Part of this work was also supported by a grant from EPSRC (EP/C510259/1) to G.R.L. The spectrometer was supported by an infrastructure grant (JIF 2000) from UK HEFCE (GR/65557). Professor Clare Grey (Stony Brook) is also thanked for helpful discussions.

References and Notes

(1) Subramanian, M. A.; Aravamudan, G.; Subba Rao, G. V. *Prog. Solid State Chem.* **1983**, *15*, 55−143.

(2) Wuensch, B. J.; Eberman, K. W.; Heremans, C.; Ku, E. M.; Onnerud, P.; Yeo, E. M. E.; Haile, S. M.; Stalick J. K.; Jorgensen, J. D. *Solid State Ionics* **2000**, *129*, 111−133.

(3) Ewing, R. C.; Weber, W. J.; Lian, J. *Appl. Phys. Rev.* **2004**, *95*, 1−23.

(4) Ringwood, A. E. *Fortschr. Mineral.* **1980**, *58*, 149−168.

(5) Chakoumakos, B. C. *J. Solid State Chem.* **1984**, *53*, 120−129.

(6) MacKenzie, K. J. D.; Smith, M. E. In *Multinuclear Solid-State NMR of Inorganic Materials*; Pergamon Press: Oxford, 2002.

(7) Heremans, C.; Stalick J. K.; Prince, E. *J. Solid State Chem.* **1995**, *117*, 108−121.

(8) Laarson, A. C.; Von Dreele, R. B. in Los Alamos National Laboratory Report LAUR, 2000.

(9) Toby, B. H. *J. Appl. Crystallogr.* **2001**, *34*, 210−213.

(10) Haile, S. M.; Weunsch, B. J.; Prince, E. *Mater. Res. Soc. Symp. Proc.* **1990**, *166*, 81−86.

(11) Kennedy, B. J. *Mater. Sci. Forum* **1996**, *228*, 753−758.

(12) Meiboom, S.; Gill, D. *Rev. Sci. Instrum.* **1958**, *29*, 688−691.

(13) Massiot, D.; Fayon, F.; Capron, M.; King, I.; Le Calve, S.; Alonso, B.; Durand, J. O.; Bujoli, B.; Gan, Z.; Hoatson, G. *Magn. Reson. Chem.* **2002**, *40*, 70−76.

(14) Grey, C. P.; Smith, M. E.; Cheetham, A. K.; Dobson, C. M.; Dupree, R. J. *Am. Chem. Soc.* **1990**, *112*, 4670−4675.

(15) Becerro, A. I.; Escudo, A.; Florian, P.; Massiot, D.; Alba, M. *J. Solid State Chem.* **2004**, *177*, 2790−2796.

(16) Dupree, R.; Smith, M. E. *Chem. Phys. Lett.* **1988**, *148*, 41−44.

(17) Harazono. T.; Watanabe, T. *Bull. Chem. Soc. Jpn.* **1997**, *70*, 2383−2388.

(18) Blumberg, W. E. *Phys. Rev.* **1960**, *119*, 79−84.

(19) Grey, C. P. DPhil Thesis, University of Oxford, 1990.

(20) Liu, Y.; Withers, R. L.; Noren, L. *J. Solid State Chem.* **2004**, *177*, 4404−4412.

(21) Kim, N.; Grey, C. P. *J. Solid State Chem.* **2003**, *175*, 110−115.

(22) Kim, N.; Grey, C. P. *Dalton Trans.* **2004**, *19*, 3048−3052.